

# Quantitative Analysis of TiB<sub>2</sub> Particles and Properties of Cu-TiB<sub>2</sub> Composite Prepared by in Situ Reaction

Xia Meng<sup>1</sup>, Feng Yi<sup>1</sup>, Tian Pei<sup>1</sup>, Song Zhaokun<sup>1</sup>, Zhao Lan<sup>2</sup>, Cai Chengyu<sup>2</sup>

<sup>1</sup> Hefei University of Technology, Hefei 230009, China; <sup>2</sup> Zhejiang Industry & Trade Vocational College, Wenzhou 325000, China

**Abstract:** Cu-TiB<sub>2</sub> composites were prepared by combining in situ reaction and hot-pressing at different temperatures after ball-milling of the mixture powders of Cu, Ti and B. The reaction process of Cu-Ti-B system was discussed. By means of XRD, SEM, EDS and XPS, it is determined that TiB<sub>2</sub> nano-particles are generated by in situ reaction in Cu-matrix. According to the calibration curve of TiB<sub>2</sub> and Cu by XRD, the concrete synthesis rate of TiB<sub>2</sub> in Cu-matrix at different sintering temperatures by external standard method was confirmed. The results show that in certain temperature range, the higher the temperature is, the higher the synthesis rate is, and the best synthesis rate of TiB<sub>2</sub> is 99.27% at 1000 °C. Cu-1.5wt%TiB<sub>2</sub> prepared at 1000 °C has the best properties, Its Vickers hardness (HV), electric conductivity (EC), flexure strength (FS), thermal expansivity (TE) and thermal conductivity (TC) at 100 °C are 125.68 MPa, 80.1 % IACS, 755.2 MPa,  $9.3 \times 10^{-6} \text{ K}^{-1}$  and 260 W/(m K), respectively.

**Key words:** Cu-TiB<sub>2</sub>; in-situ; calibration curve; property

High conductivity and high strength copper alloys have many industrial applications, including welding electrodes, rail transit contact wires, IC lead frame, continuous caster material and so on<sup>[1-4]</sup>. Owing to desired combination of electrical conductivity, thermal conductivity and mechanical properties, copper matrix composites (CMCs) have attracted so much attention in recent years. Hot-pressure sintering technique has been demonstrated to be effective in preparing CMCs in the last few decades<sup>[5-8]</sup>. By mixing reinforcing phase and copper powder directly or via an interfacial design process, ex-situ reinforced CMCs were successfully prepared. Compared to the conventional ex situ reaction, in situ reaction synthesis produces superior wetting interface between particle and matrix, and the CMCs thus prepared exhibit preferable integrated performances<sup>[9]</sup>. Accordingly, the hot-press sintering has been widely applied to prepare in-situ CMCs<sup>[10-12]</sup>.

Compared to the unreinforced copper, the improved properties of the CMCs mainly originate from the second-phase particles, such as borides (TiB<sub>2</sub>, ZrB<sub>2</sub>), carbides (TiC, SiC) and oxides (Al<sub>2</sub>O<sub>3</sub>)<sup>[13-15]</sup>. Among these

particles, TiB<sub>2</sub> is deemed to be a good candidate to reinforce CMCs because of its high elastic modulus (574 GPa), high hardness value (HV:34 GPa), good thermodynamic stability and good electrical conductivity<sup>[16]</sup>. Moreover, TiB<sub>2</sub> particles are thermodynamically stable and can easily form through in situ reactions between titanium and boron elements in copper melt<sup>[17,18]</sup>.

So far, Cu-TiB<sub>2</sub> composites prepared by in situ have many literatures<sup>[19,20]</sup>, such as the preparation methods, microstructure and mechanical properties. The content of TiB<sub>2</sub> has an important effect on the properties of the composites, but there is no research related to the conversion rate of TiB<sub>2</sub> synthesizing in-situ reaction. In order to study the effect of second phase synthesizing in-situ reaction on the properties of composite materials, quantitative calculation for the content of the second phase is of great significance.

In this paper we decided to use elemental Ti, B and Cu as raw material to in-situ synthesize TiB<sub>2</sub> reinforced phase in order to get single kind of reactive products. Powders of Cu, Ti and B blended after high-energy ball-milling were

prepared for Cu-TiB<sub>2</sub> composites by reactive hot-pressure sintering. The thermodynamic analysis of the Cu-Ti-B system, quantitative calculation of synthesis rate of TiB<sub>2</sub> particles at different sintering temperature, and the properties of the Cu-TiB<sub>2</sub> composites were emphatically carried out.

## 1 Experiment

In the present study, Cu-1.5wt%TiB<sub>2</sub> and Cu-15wt%TiB<sub>2</sub> composites were prepared in a vacuum thermocompression furnace (ZT-40-20Y) at different sintering temperatures after ball-milling the powders of Cu (purity 99.95%, 42.4 μm), Ti (purity 99.99%, 36 μm) and B (purity 99.99%, 35 μm) with a stoichiometric Ti:B of 1:2. The power mixtures were put in a stainless steel vacuum jar with alcohol. The mechanical ball-milling process was conducted for 9 h with a ball to powder ratio (BPR) of 10:1 at the milling speed of 300 r/min on planet ball grinder (QM-3SP04). Subsequently, the dried mixture powers were calcined in flowing argon atmosphere at 25 MPa in a temperature range of 600~1060 °C with heating rate for 10 °C/min and holding time for 3 h.

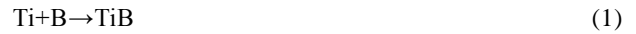
The sintered bulk samples were measured on X-ray diffractometer (D/MAX2500V, Japanese Neo Confucianism) with Cu Kα radiation at 40 kV and 150 mA, scan speed for 0.02 ° and time per step for 0.2 s to analyze the phase of the composites and prepare for the calibration curve which can be used to calculate the synthesis rate of TiB<sub>2</sub> by in situ reaction. To further analyze component of the composites, XPS (ESCALAB250, U.S.A. Thermo) was conducted to identify the valence state of elements of Cu, Ti and B. The microstructure was observed and analyzed by field emission scanning electron microscopy (FE-SEM, SU8020, Hitachi) with an energy-dispersive spectroscopy (EDS) system.

All the mechanical properties were measured at room temperature. The density of solid samples was measured by Archimedes' method. The electrical resistance was measured by a double bridge method. And the Vickers hardness test was performed on the fine polished surface by HXD-1000 tester (Shanghai second optional Ltd, China) at a load of 100 g with the dwell time of 10 s. The flexural strength of bulk Cu-TiB<sub>2</sub> specimen with dimensions of 3 mm×8 mm×35 mm was determined by the three-point bending method at Universal testing machine. The coefficient of thermal expansion of cylinder Cu-TiB<sub>2</sub> specimen with diameter of 12.8 mm were measured by thermomechanical analysis unit (TMA402F3, Netzsch) and thermal conductivity of cylinder Cu-TiB<sub>2</sub> specimen with the diameter of 6 mm by laser flash thermal analyzer(LFA457, Netzsch). In addition, in order to analyze the strengthening mechanism of Cu-TiB<sub>2</sub> composite, the fracture of solid samples after three-point test was also examined by SEM.

## 2 Results and Discussion

### 2.1 Phase transformation of Cu-Ti-B system

Fig.1 shows the phase diagrams of Cu-Ti<sup>[21]</sup> and Ti-B<sup>[22]</sup>, according to the mass ratio of copper to titanium and the atomic ratio of titanium to boron. the reactions will take place in the Cu-Ti-B system as follows:



The relationship of reaction free enthalpy and temperature by Gibbs Helmholtz equation is as follows:

$$d\left(\frac{\Delta G_T^\ominus}{T}\right) = -\frac{\Delta H_T^\ominus}{T^2} dT \quad (4)$$

In the formula, the  $\Delta H_T^\ominus$  represents the reaction heat effect,  $T$  is for the thermodynamic temperature,  $\Delta H_T^\ominus$  can be obtained by the Kirchoff formula:

$$d\Delta H_T^\ominus = \Delta C_p dT \quad (5)$$

Where  $\Delta C_p$  stands for the differences of heat capacity of the reactions,  $C_p$  changes with temperature and can be approximated by the following equation:

$$C_p = a + b10^{-3}T + c10^{-5}T^{-2} + d10^{-6}T^2 + e10^8T^{-3} \quad (6)$$

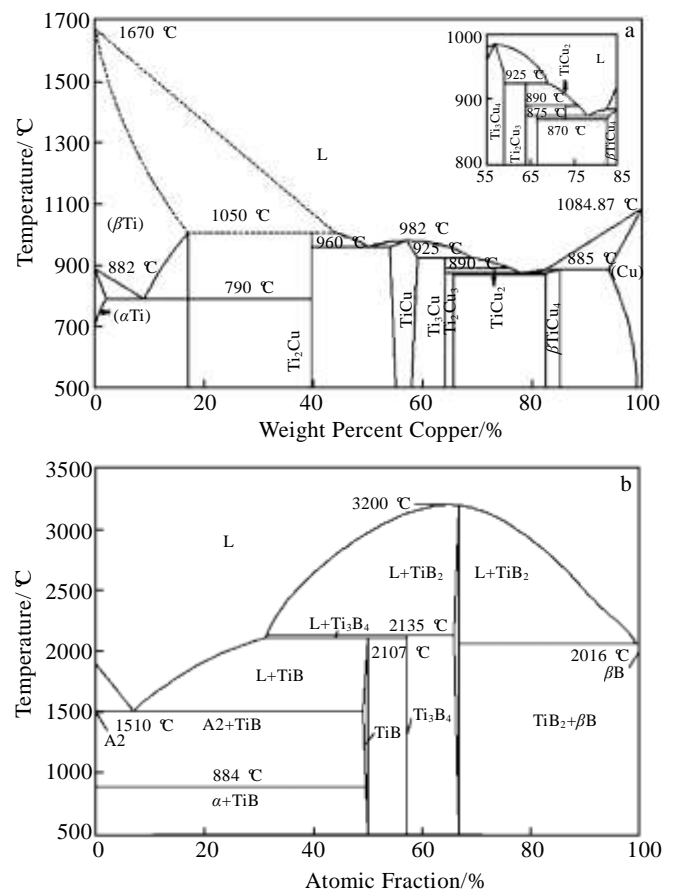


Fig.1 Phase diagrams of Cu-Ti (a) and Ti-B (b)

$$\Delta H_T^\ominus = \Delta aT + \frac{1}{2}\Delta b10^{-3}T^2 - \Delta c10^5T^{-1} + \frac{1}{3}\Delta d10^{-6}T^3 - \frac{1}{2}\Delta e10^8T^{-2} + f \quad (7)$$

$$\Delta G_T^\ominus = -\Delta aT \ln T - \frac{1}{2}\Delta b10^{-3}T^2 - \frac{1}{2}\Delta c10^5T^{-1} - \frac{1}{6}\Delta d10^{-6}T^3 - \frac{1}{6}\Delta e10^8T^{-2} + gT + f \quad (8)$$

According to consult parameters of  $a, b, c, d, e$  and the above Eqs.(4)~(8)<sup>[23]</sup>,  $\Delta a, \Delta b, \Delta c, \Delta d, \Delta e, f, g$  can be calculated as shown in Table 1.

According to Table 1 and Eq.(8), variation of free enthalpy  $\Delta G$  with temperature can be calculated in the above reaction, as shown in Fig.2.

In Fig.3, with the temperature rising, Ti and B become less and less, and  $\text{TiB}_2$  comes into being from 850 °C, which is in keeping with the result of above thermodynamic analysis. It also can be seen that with the sintering temperature rising, lattice constant of Cu ranges from 0.361 911 to 0.361 832, indicating that Ti and B which are original solid solution in the alpha-Cu precipitate gradually, and thus the alpha Cu basic restores to the original lattice constant ( $a=0.3615$ ).

Table 1 Parameters of the thermodynamics computational process

| T/K       | Phase                  | $\Delta a$ | $\Delta b$ | $\Delta c$ | $\Delta d$ | $\Delta e$ | $f$       | $g$     |
|-----------|------------------------|------------|------------|------------|------------|------------|-----------|---------|
| 298~800   | $\text{Cu}_4\text{Ti}$ | -37.45     | 4.73       | 5.56       | 0          | 0          | -94296.21 | -226.68 |
|           | TiB                    | 4.11       | -9.55      | 10.54      | 0          | -5.21      | -160443.3 | 27.07   |
|           | $\text{TiB}_2$         | -21.38     | 17.00      | 46.88      | -3.35      | -10.42     | -308329.9 | -137.69 |
| 800~1155  | $\text{Cu}_4\text{Ti}$ | -37.45     | 4.73       | 5.56       | 0          | 0          | -94296.21 | -226.68 |
|           | TiB                    | 10.55      | -14.97     | -9.52      | 0          | 0          | -165922.4 | 73.34   |
|           | $\text{TiB}_2$         | -8.50      | 6.17       | 6.75       | -3.35      | 0          | -319288.1 | -45.15  |
| 1155~1500 | TiB                    | 12.85      | -12.63     | -9.52      | 0          | 0          | -166712.1 | 89.45   |
|           | $\text{TiB}_2$         | -6.20      | 8.51       | 6.75       | -3.35      | 0          | -320077.8 | -29.04  |

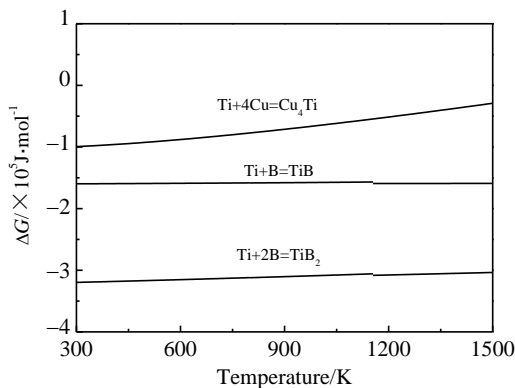


Fig.2 Relationship between  $\Delta G$  and temperature

## 2.2 Effect of temperature on the synthesis of $\text{TiB}_2$

Quantitative phase analysis method which did not add standard material to the sample when tested, usually used one kind of pure phase to be tested as standard samples, needed to make a series of external standard samples and map out the working curve, is called external standard method<sup>[24]</sup>.

Supposed that the mixture samples needed to be tested were composed of i phase and j phase,  $\mu_{mi}, \mu_{mj}$  and  $\mu_m$  are integrated mass absorption coefficient of i phase, j phase and two-phase mixtures, and  $W_i$  and  $W_j$  represent the mass percentage of i phase and j phase.

$$\begin{aligned} \mu_m &= W_i\mu_{mi} + W_j\mu_{mj} = W_i(\mu_{mi} - \mu_{mi}) + \mu_{mj} \\ &= W_j(\mu_{mj} - \mu_{mi}) + \mu_{mi} \end{aligned} \quad (9)$$

The intensity of the diffraction peak of j phase in the samples to be measured is as follow:

$$I_j = C_j \frac{W_j}{\mu_m} = \frac{c_j w_j}{W_j(\mu_{mj} - \mu_{mi}) + \mu_{mi}}, C_j = CK_j / \rho_j \quad (10)$$

The intensity of the corresponding diffraction peak of j phase in the standard samples is as follows:

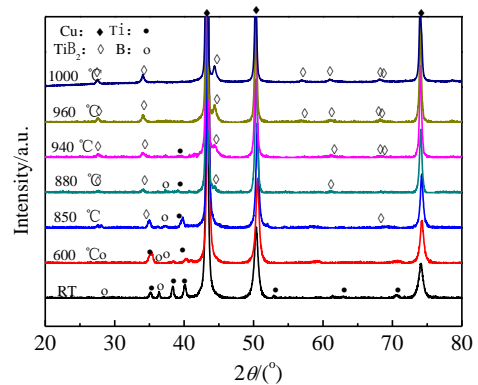


Fig.3 XRD patterns of Cu-15wt%(Ti+2B) sintered at different temperatures

$$I'_j = C_j \frac{1}{\mu_{mj}} \tag{11}$$

It can be seen from Eq.(10) and Eq.(11)

$$\frac{I_j}{I'_j} = \frac{W_j \mu_{mj}}{W_j(\mu_{mj} - \mu_{mi}) + \mu_{mi}} \tag{12}$$

The calculation process of the mass fraction of j phase in the mixture by external standard method can be summarized as the following two steps. The first step is to make a calibration curve: prepare at least more than three different proportions of two-phase (pure j phase and i phase) mixture, test their strongest diffraction peak intensity by XRD, draw calibration curve what the abscissa is the content of j phase and longitudinal coordinate is  $I_j/I_i$ , which is equivalent to Eq.(12). The second step: in the same test conditions, measure the intensity of the corresponding diffraction peak of the mixture to be measured, find the point with the same vertical coordinates in the work curve, and the horizontal coordinate value is the mass fraction of j phase in the mixture.

So in order to calculate the synthesis rate of  $TiB_2$ , seven  $Cu-xwt\%TiB_2$  ( $x=2.5, 5, 10, 15, 20, 25, 30$ ) samples with Cu powder and pure  $TiB_2$  (99.9%, 3.8  $\mu m$ ) were prepared by sintering at 980  $^{\circ}C$ . Calculate the peak intensity ratio of  $TiB_2$  to Cu under the different mass fraction of  $TiB_2$  by XRD as show in Table 2, then make calibration curve using the mass fraction of  $TiB_2(TiB_2\%)$  as the abscissa and the peak intensity ratio of  $TiB_2$  to Cu ( $I_{TiB_2}/I_{Cu}$ ) as the ordinate as shown in Fig.4a. In addition,  $Cu-ywt\%TiB_2$  ( $y=2.59, 5.34, 8.23, 14.48, 21.47, 29.35, 38.29$ ) composites were random prepared in the same conditions again, according to the above method to draw another calibration curve, as shown in Fig.4b. The two calibration curves were nearly superposition, which indicated that the curve was with high confidence level. At last, Fig.4b was chosen as the work curve to calculate the mass fraction of  $TiB_2$  at different sintering temperatures. And the equation was gained by making calibration curve of Cu -  $TiB_2$  as follows:

$$\frac{I_a}{I_b} = 0.0132 + 0.377W_a + 0.8919W_a^2 \tag{13}$$

where,  $I_a$  and  $I_b$  are the integrated diffraction intensity of  $TiB_2$  (101) peak and Cu (111) peak, respectively, and  $W_a$  represents the mass percentage of  $TiB_2$ .

Fig.5 shows XRD patterns of the samples calcined in the temperature range of 940~1060  $^{\circ}C$  from the milled powders of  $Cu-15wt\%(Ti+2B)$ . Obviously, it is clear that there are Cu phase and  $TiB_2$  second phase in the samples. By external standard method, Fig.5 was applied to calculate the mass fraction of  $TiB_2$  in the sample. Firstly test the strongest diffraction peak intensity of  $TiB_2$  and Cu under the above measure conditions by XRD as shown in Table 3, and then the

**Table 2 Peak intensity of the mixtures of different contents of  $TiB_2$  and Cu**

| $TiB_2$ content/<br>wt% | $I_{TiB_2}$ (avg) | $I_{Cu}$ (avg) | $I_{TiB_2}/I_{Cu}$ (avg) |
|-------------------------|-------------------|----------------|--------------------------|
| 2.5                     | 25037             | 1411497        | 0.018                    |
| 5                       | 50669             | 1314626        | 0.039                    |
| 10                      | 75367             | 1204749        | 0.063                    |
| 15                      | 100685            | 1124018        | 0.09                     |
| 20                      | 121906            | 1003517        | 0.121                    |
| 25                      | 143529            | 892083         | 0.161                    |
| 30                      | 163137            | 779849         | 0.209                    |
| 2.59                    | 29385             | 1363711        | 0.022                    |
| 5.34                    | 43501             | 1303119        | 0.033                    |
| 8.23                    | 62971             | 1214559        | 0.05                     |
| 14.48                   | 96218             | 1103959        | 0.087                    |
| 21.47                   | 127395            | 900106         | 0.14                     |
| 29.35                   | 153851            | 795648         | 0.193                    |
| 38.29                   | 184418            | 619615         | 0.298                    |

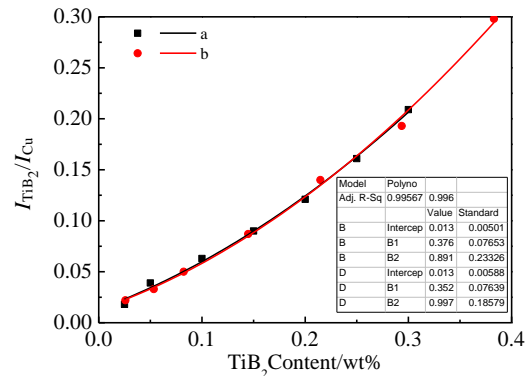


Fig.4 Work curve of  $TiB_2$  and Cu: (a)  $Cu-xwt\%TiB_2$  ( $x=2.5, 5, 10, 15, 20, 25, 30$ ); (b)  $Cu-ywt\%TiB_2$  ( $y=2.59, 5.34, 8.23, 14.48, 21.47, 29.35, 38, 29$ )

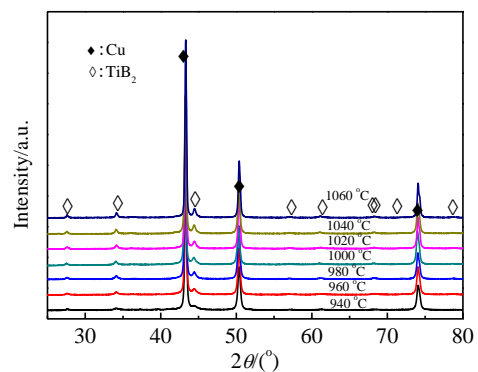


Fig.5 XRD pattern of  $Cu-15wt\%(Ti+2B)$  sintered at different temperatures

**Table 3 Peak intensity of Cu-TiB<sub>2</sub> composites**

| T/°C | I <sub>TiB<sub>2</sub></sub> (avg) | I <sub>Cu</sub> (avg) | I <sub>TiB<sub>2</sub></sub> /I <sub>Cu</sub> (avg) |
|------|------------------------------------|-----------------------|---|
| 940  | 54574                              | 973437                | 0.05604   |
| 960  | 73253                              | 1004153               | 0.07295   |
| 980  | 79066                              | 972401                | 0.08131   |
| 1000 | 88729                              | 995389                | 0.08914   |
| 1020 | 90343                              | 1025925               | 0.08806   |
| 1040 | 91499                              | 1047331               | 0.08736   |
| 1060 | 91529                              | 1051936               | 0.08701   |

mass fraction of TiB<sub>2</sub> samples can be checked in Fig.5, which was the value of the horizontal coordinate corresponding to the same vertical coordinate.

From Fig.6, it can be seen that with the temperature increasing, atoms proliferated more fully and it leads to the synthesis rate of TiB<sub>2</sub> increasing gradually. As temperature further increases, the impact of the sintering temperature on the synthesis rate of TiB<sub>2</sub> changes little because of Ti and B almost completely transform into TiB<sub>2</sub>.

**2.3 Microstructure and properties of Cu-TiB<sub>2</sub> composites**

It is observed that the TiB<sub>2</sub> particles synthesized by in situ in the matrix are cubic and spherical in form and the

size of the TiB<sub>2</sub> particles ranges from 50 to 200 nm as shown in Fig.7a and Fig.7b, which is much lower than that of ex situ particles in discontinuously reinforced composites. What's more, take measures of line-scanning on the samples, it can be seen that the peak position of Ti is the same as B elements in the black particles, which is opposite of Cu element in Fig.7c, illustrating that the TiB<sub>2</sub> particles are generated in the in situ reaction in keep with the result of above analysis.

Fig.8 shows XPS spectra of Cu-TiB<sub>2</sub> composite at 1000 °C. The spectrum displays the spin-orbit splitting characteristic of Cu 2p, Ti 2p and B 1s levels. The intensity ratio of the Cu 2p<sub>3/2</sub> and Cu 2p<sub>1/2</sub> peaks is constrained to be

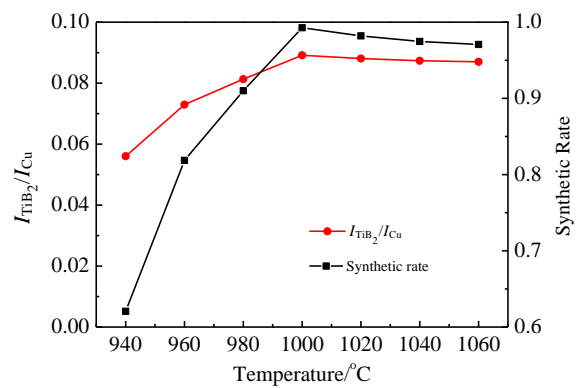


Fig.6 Synthetic rate curves of TiB<sub>2</sub>

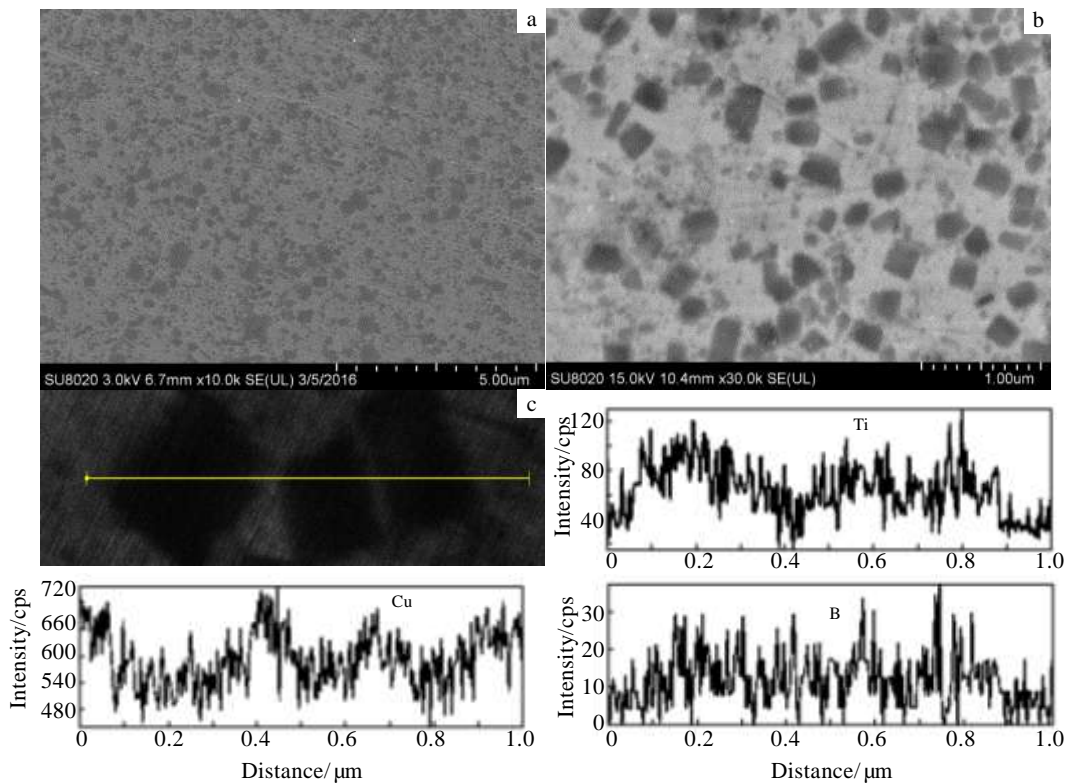
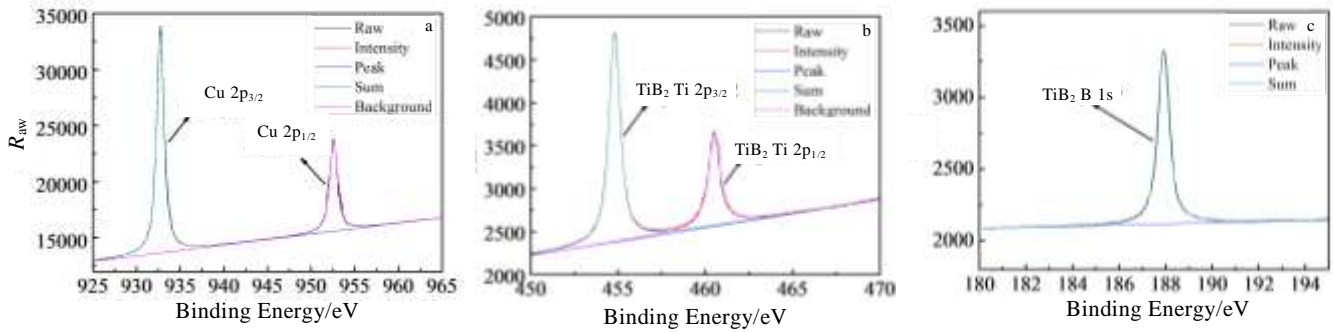


Fig.7 SEM images (a, b) and EDS element line scanning (c) of Cu-TiB<sub>2</sub> composite

Fig.8 XPS spectra of Cu-TiB<sub>2</sub> composite at 1000 °C: (a) Cu 2p, (b) Ti 2p, and (c) B 1s**Table 4 Properties of Cu-TiB<sub>2</sub> composites prepared by different methods**

| Material                                | Methods            | RD/%  | Hardness, HV/MPa | EC /% IACS | TS /MPa | FS /MPa | TE / $\times 10^{-6} \text{ K}^{-1}$ | TC /W (m K) <sup>-1</sup> |
|---|--------------------|-------|------------------|------------|---------|---------|--------------------------------------|---------------------------|
| Cu                                      | -                  | 99.8  | 60               | 99.9       | 206     | -       | 17.5                                 | 397                       |
| Cu-1.5%TiB <sub>2</sub>                 | Solid-solid(HP)    | 98.28 | 125.68           | 80.1       | 560     | 755.2   | 9.3                                  | 260                       |
| Cu-2%TiB <sub>2</sub> <sup>[11]</sup>   | Solid-solid(MA)    | -     | -                | 78.4       | 545     | -       | -                                    | -                         |
| Cu-0.5%TiB <sub>2</sub> <sup>[29]</sup> | Solid-liquid(RSD)  | -     | -                | 63.5       | 410     | -       | -                                    | -                         |
| Cu-2.6%TiB <sub>2</sub> <sup>[30]</sup> | Liquid-liquid(DBM) | -     | -                | 76         | 675     | -       | -                                    | -                         |

2:1 during the fitting procedure and so does Ti. Linear background is used during the fitting procedure. The peak of Ti 2p at about 454.7 and 460.4 eV as reported for TiB<sub>2</sub><sup>[25,26]</sup>. And only one peak of B can be fitted at around 187.9 eV as reported for TiB<sub>2</sub><sup>[27,28]</sup>. It can be seen that Cu element without forming the other compound, Ti element and B element almost exist in the form of TiB<sub>2</sub>. The result is the same as XRD analysis, which further proved that the Ti powder and B powder synthesized TiB<sub>2</sub> in situ.

From Table 4, it can be seen that Cu-TiB<sub>2</sub> composite prepared by hot-pressing(HP) at 1000 °C contrast with pure copper significantly improves the stability and increases hardness, while the electrical conductivity decreases slightly. And its electric conductivity and tensile strength are higher than that of Cu-TiB<sub>2</sub> composites manufactured by mechanical alloying (MA) and reaction spray deposition forming process (RSD). Cu-2wt%TiB<sub>2</sub> prepared by MA requires long time for 25 h though with low temperature of 890 °C<sup>[11]</sup>. Cu-0.5wt%TiB<sub>2</sub> prepared by RSD demanded high temperature of 1400~1500 °C; furthermore, it had segregation and incompleting reaction<sup>[29]</sup>. Although Cu-5vol%TiB<sub>2</sub> (equal to Cu-2.6wt%TiB<sub>2</sub>) prepared by double beam melts(DBM) had relatively good properties, it not only needed to react at high temperature, but also the size and distribution of TiB<sub>2</sub> were not easy to control<sup>[30]</sup>.

### 3 Conclusions

1) By the external standard method, TiB<sub>2</sub> nanoparticles generated by in situ reaction in Cu-matrix are determined. The amount of TiB<sub>2</sub> in the samples is calculated by the ratios of the peak intensities of TiB<sub>2</sub> and Cu obtained from XRD studies. As sintering temperature increases, the synthesis rate of TiB<sub>2</sub> becomes higher, and the best synthesis rate is up 99.27% at 1000 °C.

2) By composite technology of in situ reaction and hot-pressure sintering, high-performance composites Cu-TiB<sub>2</sub> is produced, and the size of the enhancement TiB<sub>2</sub> particle is about 50~200 nm, which is of uniform distribution without segregation.

3) The best comprehensive performance of Cu-1.5wt% TiB<sub>2</sub> composites is obtained by hot-pressing sintering at 1000 °C, including the density 98.28%, conductivity 80.1%IACS, micro Vickers hardness (HV) 125.68 MPa, and bending strength 755.2 MPa, thermal expansion coefficient  $9.3 \times 10^{-6} \text{ K}^{-1}$  at 100 °C and thermal conductivity 260 W (m K)<sup>-1</sup> at 100 °C.

### References

- 1 Lu K. *Science*[J], 2010, 328: 319
- 2 Tan Yuehua, Yan Bo, Gao Ge et al. *Journal of Wuhan*

- University of Technology-Mater Sci Ed[J], 2006, 21(3): 69 (in Chinese)
- 3 Machlin E S. *An Introduction to Aspects of Thermodynamics and Kinetics Relevant to Materials Science*[M]. New York: Gyro Press, 2007: 159
  - 4 Zhai W, Wang W L, Geng D L et al. *Acta Mater*[J], 2012, 60(19): 6518
  - 5 Uddin S M, Mahmud T, Wolf C et al. *Composites Science and Technology*[J], 2010, 70: 2253
  - 6 Wang G S, Fan G H, Geng L et al. *Materials Science and Engineering A*[J], 2013, 571: 144
  - 7 Schubert T, Brendel A, Schmid K et al. *Composites Part A*[J], 2007, 38: 2398
  - 8 Cui G, Bi Q, Zhu S et al. *Tribology International*[J], 2012, 53: 76
  - 9 Fan Z, Miodownik A P, Chandrasekaran L et al. *Journal of Materials Science*[J], 1994, 29: 1127
  - 10 Ngai T L, Zheng W, Li Y. *Progress in Natural Science Materials International*[J], 2013, 23: 70
  - 11 Dong S J, Zhou Y, Shi Y W et al. *Metallurgical and Materials Transactions A*[J], 2002, 33: 1275
  - 12 Lu J, Shu S, Qiu F et al. *Materials & Design*[J], 2012, 40: 157
  - 13 Bagheri G A. *Journal of Alloys and Compounds*[J], 2016, 676: 120
  - 14 Tu J P, Wang N Y, Yang Y Z et al. *Materials Letters*[J], 2002, 52 : 448
  - 15 Tayeh T, Douin J, Jouannigot S et al. *Materials Science and Engineering A*[J], 2014, 591: 1
  - 16 Basu S N, Hubbard K M, Hirvonen J P et al. *Spring Meeting of the Materials Research Society*[C]. San Francisco: Materials Research Society, 1990
  - 17 Dallaire S, Legoux J G. *Materials Science and Engineering A*[J], 1994, 183(1-2): 139
  - 18 Guo M X, Wang M P, Shen K et al. *Journal of Alloys and Compounds*[J], 2008, 460: 585
  - 19 Shen Yanwei, Li Xianfeng, Hong Tianran et al. *Materials Science and Engineering A*[J], 2016, 655: 265
  - 20 Jiang Yihui, Wang Chen, Liang Shuhua et al. *Materials Characterization*[J], 2016, 121: 76
  - 21 Osório Wislei R, Freire Celia M, Caram Rubens et al. *Electrochimica Acta*[J], 2012, 77: 189
  - 22 Witusiewicz V T, Bondar A A, Hecht U et al. *Journal of Alloys and Compounds*[J], 2016, 655: 336
  - 23 Ye Dalun, Hu Jianhua. *Practical Handbook of Inorganic Thermodynamic*[M]. Beijing: Metallurgical Industry Press, 2002: 106 (in Chinese)
  - 24 Jin Yong, Sun Xiaosong, Xue Qi. *X-Ray Diffraction Analysis Technique*[M]. Beijing: National Defense Industry Press, 2008: 195 (in Chinese)
  - 25 Ding Hongyan, Zhou Guanghong, Liu Tao et al. *Tribology International*[J], 2015, 89: 62
  - 26 Benko E, Barr T L, Hardcastle S, Hoppe E et al. *Ceramics International*[J], 2001, 27: 637
  - 27 Chi Haitao, Jiang Longtao, Chen Guoqin et al. *Materials and Design*[J], 2015, 87: 960
  - 28 Higdon C, Cook B, Harringa J et al. *Wear*[J], 2011, 271: 2111
  - 29 Tu J P, Rong W, Guo S Y et al. *Wear*[J], 2003, 255: 832
  - 30 Lee A K, Sanchez-galdera L E, Oktay S T et al. *Advanced Material Processes*[J], 1995, 8: 31

## 原位合成 TiB<sub>2</sub> 的定量计算及 Cu-TiB<sub>2</sub> 复合材料性能的研究

夏梦<sup>1</sup>, 凤仪<sup>1</sup>, 田沛<sup>1</sup>, 宋焯坤<sup>1</sup>, 赵岚<sup>2</sup>, 蔡承宇<sup>2</sup>

(1. 合肥工业大学, 安徽 合肥 230009)

(2. 浙江工贸职业技术学院, 浙江 温州 325000)

**摘要:** 以 Ti 粉、B 粉和 Cu 粉为原材料, 球磨后, 采用热压法原位合成 Cu-15%TiB<sub>2</sub> (质量分数) 复合材料。并详细讨论了 Cu-Ti-B 体系的反应过程。通过 XRD、SEM、EDS、XPS 等手段, 确定了 Ti 和 B 在 Cu 基体中原位合成了 TiB<sub>2</sub>, 并利用 XRD 制作 TiB<sub>2</sub> 和 Cu 的定标曲线, 采用外标法计算出不同烧结温度下 TiB<sub>2</sub> 的合成率。结果表明, 在一定的温度范围内, 温度越高, 合成率越高, 在 1000 °C 时 TiB<sub>2</sub> 的合成率可达 99.27%。并测试 Cu-1.5%TiB<sub>2</sub> 块状试样的维氏硬度, 电导率和三点弯曲强度, 分别为 125.68 MPa、80.1% IACS 和 755.2 MPa, 在 100 °C 时的热膨胀系数和导热系数分别为  $9.3 \times 10^{-6} \text{ K}^{-1}$  和 260 W/(m K)。

**关键词:** Cu-TiB<sub>2</sub>; 原位; 定标曲线; 性能

作者简介: 夏梦, 女, 1990 年生, 硕士生, 合肥工业大学材料科学与工程学院, 安徽 合肥 230009, 电话: 0551-62904715, E-mail:

XiaMeng726@163.com